Final Technical Report

from

Department of Materials Science and Engineering
Stanford University
Stanford, CA 94305 - 2205

to

Department of the Air Force
AFOSR/NA
801 North Randolph Street
Room 732
Arlington, VA 22203 - 1977

Attention: Dr. Craig S. Hartley, Ph.D., P.E.
Program Manager for Metallic Materials

on

FUNDAMENTAL MECHANISMS OF DEFORMATION AND FRACTURE

IN

HIGH-STRENGTH BULK METALLIC GLASS ALLOYS AND THEIR COMPOSITES

Principal Investigator:

Reinhold H. Dauskardt
Stanford University

AFOSR Grant No. AF-F49620-98-1-0260-P00003

April 2001

STANFORD UNIVERSITY

REPORT DOCUMENTATION PAGE

AFRL-SR-BL-TR-01-

0402

1. AGENCY USE ONLY *(Leave blank)*	2. REPORT DATE	3. RE
	APRIL 2001	FINAL TECHNICAL REPORT 1 Feb 98 - 31 Jan 01

4. TITLE AND SUBTITLE
FUNDAMENTAL MECHANISMS OF DEFORMATION AND FRACTURE IN HIGH-STRENGTH BULK METALLIC GLASS ALLOYS AND THEIR COMPOSITES

5. FUNDING NUMBERS
F49620-98-1-0260

2306/AX
61102F

6. AUTHOR(S)
REINHOLD DAUSKARDT

7. PERFORMING ORGANIZATION NAME(S) AND ADDRESS(ES)
STANFORD UNIVERSITY
STANFORD, CA 94305-2205

8. PERFORMING ORGANIZATION REPORT NUMBER

9. SPONSORING/MONITORING AGENCY NAME(S) AND ADDRESS(ES)
AIR FORCE OFFICE OF SCIENTIFIC RESEARCH
801 N. RANDOLPH STREET, ROOM 732
ARLINGTON, VA 22203-1977

10. SPONSORING/MONITORING AGENCY REPORT NUMBER

11. SUPPLEMENTARY NOTES

12a. DISTRIBUTION AVAILABILITY STATEMENT
APPROVED FOR PUBLIC RELEASE, DISTRIBUTION IS UNLIMITED

12b. DISTRIBUTION CODE

13. ABSTRACT *(Maximum 200 words)*

The recent development of bulk metallic glasses (BMG's) offers the potential for metallic material systems with dramatically improved mechanical properties. Tensile strengths of 2 Gpa and toughnesses of up to 55 Mpav.m have been reported. These high strength and toughness values are accompanied by remarkably little plastic deformation. Until recently, little work has been undertaken to elucidate the fundamental deformation and fracture mechanisms of these alloys. This technical report describes a three year program of study designed to characterize the mechanisms of deformation, fracture and fatigue of a Zr-based BMG under a range of stress state, environmental and fatigue loading conditions.

14. SUBJECT TERMS	15. NUMBER OF PAGES
	13
	16. PRICE CODE

17. SECURITY CLASSIFICATION OF REPORT	18. SECURITY CLASSIFICATION OF THIS PAGE	19. SECURITY CLASSIFICATION OF ABSTRACT	20. LIMITATION OF ABSTRACT
U	U	U	

ABSTRACT

The recent development of *bulk* metallic glasses (BMG's) offers the potential for metallic material systems with dramatically improved mechanical properties. Tensile strengths of 2 GPa and toughnesses of up to 55 MPa$\sqrt{m}$ have been reported. These high strength and toughness values are accompanied by remarkably little plastic deformation. Until recently, little work has been undertaken to elucidate the fundamental deformation and fracture mechanisms of these alloys. This technical report describes a three year program of study designed to characterize the mechanisms of deformation, fracture and fatigue of a Zr-based BMG under a range of stress state, environmental and fatigue loading conditions.

RESEARCH OBJECTIVE

The objective of our program was to provide a fundamental understanding of the mechanical and fracture properties of amorphous metallic alloys and to provide a rational basis for improving reliability and predicting long term life. Our approach has been centered around systematic efforts to characterize and understand yielding, constitutive behavior and plasticity under multiaxial loading and the fracture toughness, fatigue crack-growth resistance and creep behavior under selected environmental and temperature conditions.

OBJECTIVE OF AFOSR PROGRAM

The objective of our program was to provide a fundamental understanding of the mechanical and fracture properties of amorphous metallic alloys and to provide a rational basis for improving reliability and predicting long term life. Our approach has been centered around systematic efforts to characterize and understand yielding, constitutive behavior and plasticity under multiaxial loading and the fracture toughness, fatigue crack-growth resistance and creep behavior under selected environmental and temperature conditions.

PROGRESS

Plasticity Studies

Although the mechanical behavior of metallic glasses has been extensively studied, the precise nature of the deformation mechanisms in these amorphous metals remains unclear. Flow in metallic glasses is extremely inhomogeneous at high stresses and low temperatures; the inhomogeneous nature of the deformation is manifested in the serrated plastic flow exhibited by a metallic glass sample tested in uniaxial compression. Serrated flow is characterized by repeating cycles of a sudden stress drop followed by elastic reloading as shown in Figure 1. Flow in metallic glasses appears to be related to a local change in viscosity in shear bands near planes of maximum shear; there are two hypotheses as to why this may be the case. The first suggests that, during deformation, the viscosity within the shear bands decreases due to the formation of free volume, which in turn decreases the density of the glass [1]. The second hypothesis contends that local adiabatic heating up to the glass transition temperature, or even the melting temperature, occurs, decreasing the viscosity by several orders of magnitude [2]. In both cases, a change in viscosity localizes the deformation and leads to inhomogeneous flow. The aim of this work was to differentiate between these two deformation mechanisms by studying serrated flow in detail.

We have studied the serrated plastic flow observed in $Zr_{40}Ti_{14}Ni_{10}Cu_{12}Be_{24}$ and $Pd_{40}Ni_{40}P_{20}$ bulk metallic glass alloys tested in uniaxial compression [3,4,5]. Quantitative measurements with sufficient temporal resolution to record the fine–scale structure of the data have been made. These data are used to predict temperature increases in single shear bands due to local adiabatic heating caused by the work done on the sample during plastic deformation. Since the predicted temperature increases are on the order of only a few degrees Kelvin (or a few tens of degrees if flow is assumed to occur in a discrete zone of material along the slip band), it seems unlikely that localized heating is the primary cause of flow localization. Instead, changes in viscosity associated with increased free volume in the shear band seem more consistent with experiment. Substantial shear band heating is, however, predicted for final failure, as corroborated by evidence of melting on the fracture surface.

Microscopy of metallic glass samples tested in uniaxial compression indicates that the shear bands are oriented at an angle of 42 degrees to the loading axis as shown in Figure 2. This deviation from the plane of maximum resolved shear suggests that the normal stress acting across the shear plane influences the deformation of metallic glasses. Such a normal stress dependence supports the free volume theory of deformation.

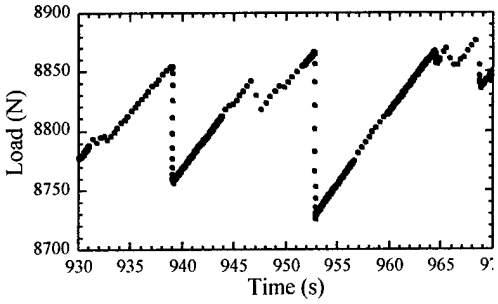

Figure 1. Load as a function of time in serrated flow region in $Pd_{40}Ni_{40}P_{20}$ tested in uniaxial compression.

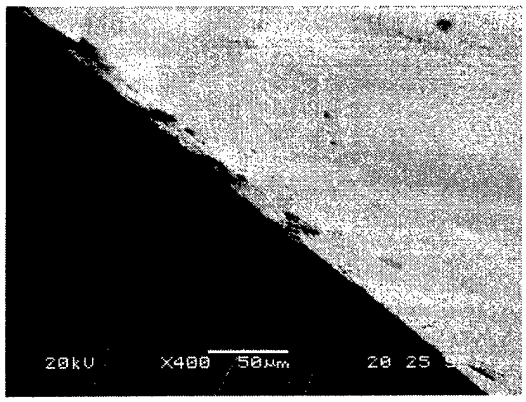

Figure 2. Scanning electron micrograph of shear bands in a $Zr_{40}Ti_{14}Ni_{10}Cu_{12}Be_{24}$ sample tested in uniaxial compression. The shear bands are perpendicular to the loading axis on one side of the sample and are oriented at an angle of 42 degrees to the loading axis on the adjacent side of the sample.

Stress State and Temperature Effects on Shear Band Formation

In an effort to study the viscosity decrease associated with shear band formation and plasticity, we have included the effects of temperature and stress state in a model for flow localization [6,7]. The effect of a superimposed compressive and tensile mean stress in this model is in excellent agreement with experimental results, as shown in Figure 3. For tensile stress states, experimental results indicate that failure occurs at a critical mean stress of ~0.9 GPa. The model includes an elastic response of the free volume to the imposed mean stress that is asymmetric about zero mean stress. By determining the dilatation due to this mean stress, and comparing this with the dilatation due to thermal expansion, we have shown that a mean stress of 0.9 GPa is equivalent to a temperature increase of 260 K. That is, the free volume dilatation at the critical mean stress is almost the same as that due to heating to the glass transition temperature. This has a significant impact on the viscosity of the material.

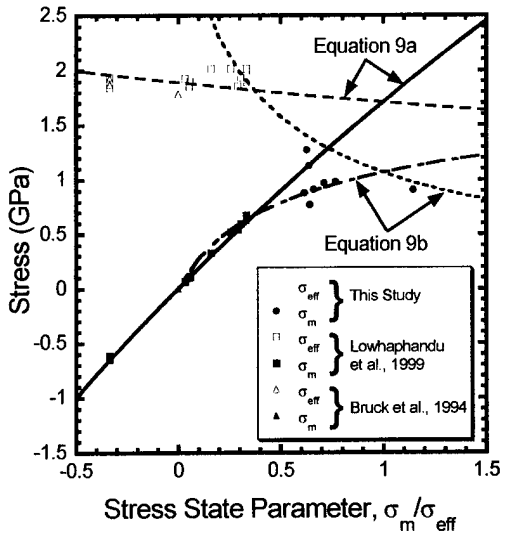

Figure 3. Correlation between the free volume model developed in this study and the mean and effective stresses measured for a range of stress states. Eqn. 9a and 9b refer to tensile and compressive mean stresses, respectively [7].

The first direct experimental evidence of the limited extent of adiabatic heating in the plastic zone ahead of a Mode I crack under nominal loading rates was also determined [8]. Several crack growth sequences were captured using a thermal imaging system as the crack propagated and arrested. A representative image is presented in Figure 4. A maximum temperature of 22.5 K above ambient was measured near the initial crack tip. The crack extended ~0.9 mm by unstable fracture until arrest in a time of less than 20 ms before the image shown. Using a heat dissipation model, we estimate that the fracture occurred 5 ms before the image shown, and the lower bound crack velocity was 175 mm/s. Additionally, the dissipation model indicates that the crack tip temperature change at initiation was ~54.2 K. This is in excellent agreement with the Rice and Levy model which indicates that the temperature rise at a crack propagating at 175 mm/s is 56.5 K for an applied stress intensity of 21 MPa$\sqrt{m}$.

While these temperature rises are insufficient to cause localized melting, it is evident from the fractography that softening did occur, causing the familiar vein patterns. More recent thermal images obtained during Mode II loading are shown in Figure 5 [9]. Small (~ 0.5 K) transient temperature increases were repeatedly measured ahead of the crack tip along the plane of maximum shear, beginning at K_{II} = 77.3 MPa$\sqrt{m}$. However, there was no apparent crack growth coincident with these heating events. The temperature increases were associated with shear band propagation from the crack tip and subsequent arrest. Unstable fracture occurred at K_{II} = 79.5 MPa$\sqrt{m}$ along the same plane. A maximum temperature of 17.8 K was measured in this case. The results suggest that reactivation of the same shear band occurred and is associated with a change in glass structure along the shear band. Surface sensitive positron annihilation studies are proposed to elucidate the nature of the change.

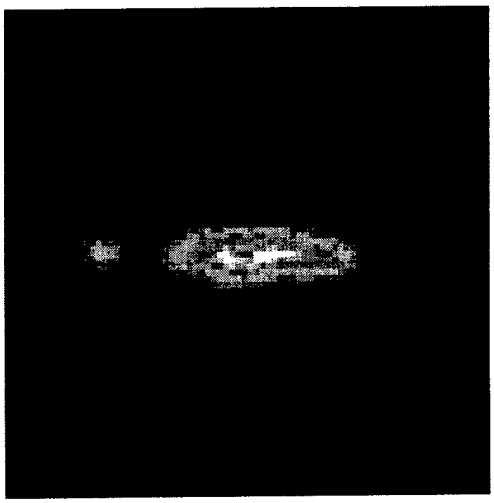

Figure 4: Thermal image after a fracture event. The image is 7 mm x 7 mm, the stress intensity at initiation was 20.8 MPa$\sqrt{m}$, and the maximum temperature was 22.5 K [8].

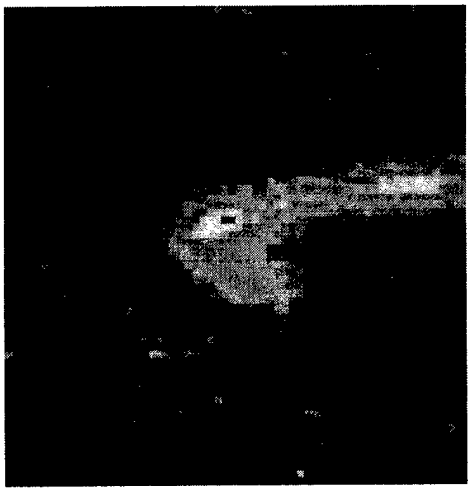

Figure 5: Thermal image of a shear band ahead of a crack tip loaded under Mode II conditions. The image is 1.92 mm x 1.92 mm. The maximum temperature rise associated with the shear band formed at K_{II} = 77.3 MPa$\sqrt{m}$ was ~ 0.5 K [9].

Flow Models including Temperature and Stress State Effects

As described above, the effects of mean stress can be included in modified flow relationships that provide good agreement with measured flow properties. We have also begun to explicitly include the effect of adiabatic heating from plastic flow in the fundamental flow relationships for metallic glasses (Fig. 6). Preliminary calculations for homogeneous flow that include heating in the shear band and subsequent conduction of the heat to the adjacent material indicate that the softening stress may be decreased by up to five percent, with the effect being more pronounced at higher strain rates and higher amounts of initial free volume. Heating causes temperature rises on the order of ten degrees at the peak stress for the case of homogeneous flow, but only a few degrees in the case of inhomogeneous flow (Fig. 7). More significant increases in temperature occur as the bulk metallic glass continues to soften. These models are in the process of being extended to include localized inhomogeneous flow, where the flow is localized to a shear band and heat is conducted from the shear band. The intent is to provide flow relationships that can more accurately predict the onset of catastrophic softening and the resulting flow behavior of the metallic glass.

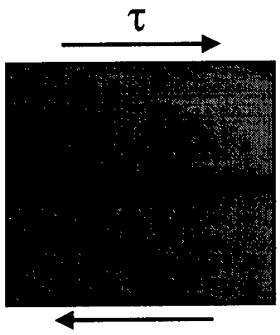

Figure 6: Shear band heat conduction model.

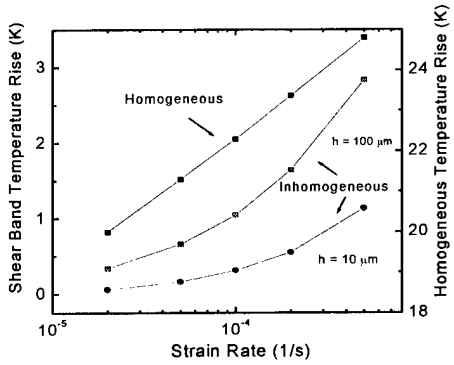

Figure 7: Temperature increases at the peak stress (catastrophic softening stress).

Characterization of Free Volume with Positron Annihilation Spectroscopy

The free volume of metallic glasses has a significant effect on plastic flow and other atomic relaxation processes although understanding of the nature and distribution of the atomic scale free volume in amorphous metals is lacking. We have directly characterized free volume changes in a bulk metallic glass using positron annihilation spectroscopy techniques following plastic straining and cathodic charging with atomic hydrogen [10,11]. First, positron lifetime in the solid, which is a function of the electron density and thus the amount of "open space" in the material, was found to increase as predicted by free volume models for plastic flow (Fig. 8). Further, hydrogen charging decreases lifetime, indicating a decrease in free volume. This is consistent with hydrogen occupying larger open volume sites and displacing the positron into smaller open volume regions. Hydrogen charging has been shown to increase both the glass transition temperature and hardness of the metallic glass, indicating that the atomic mobility has been suppressed [12]. To the best of our knowledge, these are the first direct measures of free volume changes following straining or hydrogen charging.

The momentum distribution of the γ-radiation resulting from positron annihilation in the solid provides additional information about the local chemical environment of the annihilation site. When compared with the stoichiometric proportions of the constituent elements, these results indicate that the free volume sites are primarily associated with the larger Zr and Ti atoms, as shown in Figure 9. Additionally, it is clear that plastic straining causes a slight chemical reordering around the free volume sites. The amount of Zr at the free volume sites increases by 2-4% at the expense of Ti. The Zr contribution to the annihilation radiation increased dramatically in a fully crystallized sample, while the Ti contribution again showed a complimentary decrease. This significant reordering is expected since the alloy phase separates during the crystallization process and the type of positron annihilation site changes (e.g. free volume versus grain boundary). As demonstrated, PAS provides a unique characterization technique for studying free volume in metallic glasses and will be used in the continuation program.

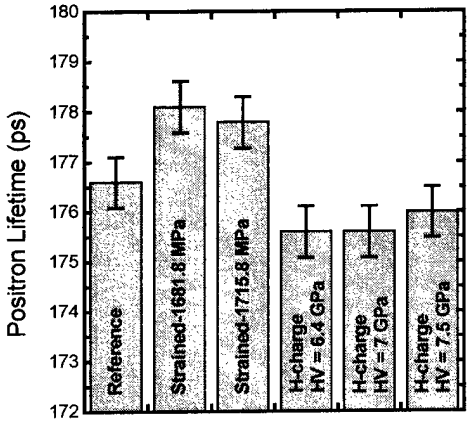

Figure 8: Positron lifetime data for prestrained and hydrogen charged bulk metallic glass samples. The longer lifetime in the strained samples is consistent with a free volume increase relative to the control sample.

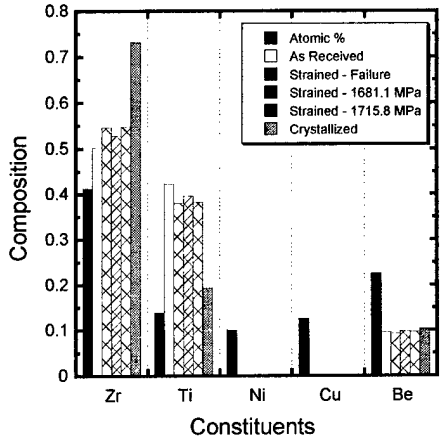

Figure 9: The elemental contribution to the momentum spectra are compared with the atomic composition of the bulk metallic glass alloy. Nickel and copper were not needed to achieve a good fit to the experimental spectra.

Fracture Toughness and Crack Tip Plasticity

Early examination of the fracture behavior of the bulk metallic glass indicated that the fracture toughness is 15-20 MPa$\sqrt{m}$ [8]. However, by utilizing a geometry which tends to stabilize shear band formation and distribute plastic deformation at the crack tip, it is possible to achieve fracture toughnesses in excess of 80 MPa$\sqrt{m}$ [13]. The distributed damage zone is shown in Figure 10. Shear bands ahead of the crack tip form an array of branched cracks. By modeling these branches as an array of parallel cracks under the influence of the stress field associated with the main crack tip, we have shown that the crack branches propagate at a local stress intensity of ~10 MPa$\sqrt{m}$, in agreement with earlier single crack measurements and the Taylor meniscus instability model.

The ability to form stable damage zones is the key to increasing the toughness and reliability of bulk metallic glasses. The incorporation of second phases is a powerful method for blocking shear band propagation and increasing stability. Preliminary studies of a bulk metallic glass composites with a crystalline Zr-Ti-Nb β-phase formed *in situ* have increased fracture toughness values of ~ 35 MPa√m with extensive stable crack growth observed during testing (Fig. 11). In the continuation program, we propose to systematically investigate the fracture toughness and model the toughening mechanism for a range of BMG composites.

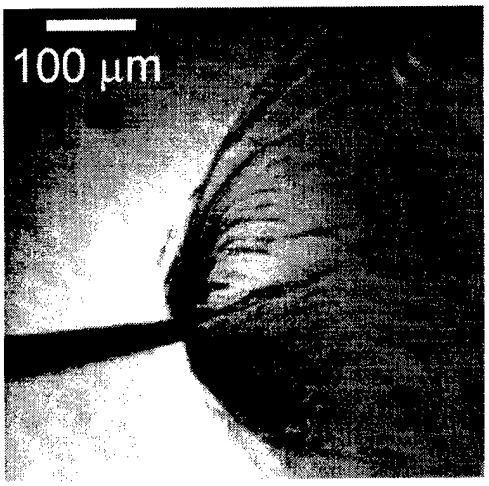

Figure 10: *In-situ* image of crack tip branching at an applied stress intensity of 81 MPa√m. The displacement rate was 0.5 μm/s.

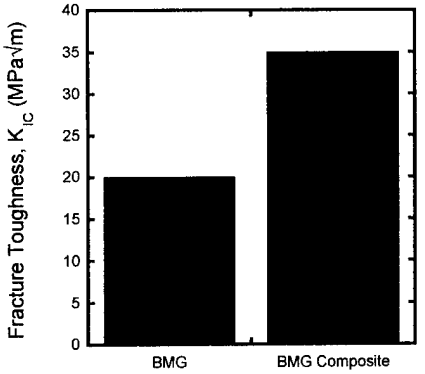

Figure 11: Comparison of fracture toughness for the bulk metallic glass (BMG) and a BMG matrix composite with 25 vol.% crystalline Zr-Ti-Nb β phase formed *in situ*.

Fatigue Behavior

The fatigue behavior of bulk metallic glasses and their composites are of particular concern for structural applications. Previous work has indicated that the BMG's have low fatigue crack-growth threshold values and fatigue limits [14]. Fatigue crack-growth rates appear to be dominated by a fatigue mechanism that depends on the near tip plastic displacements, giving rise to a crack growth exponent of ~ 2. In the present program, fatigue behavior has been assessed using both fatigue-life and crack-growth studies. Studies include both monolithic and composite BMG materials. For the initial composite materials examined, fatigue crack-growth properties were found to be similar to the monolithic BMG. The reason is that the Ti-Zr-Nb ductile second phase does not exhibit

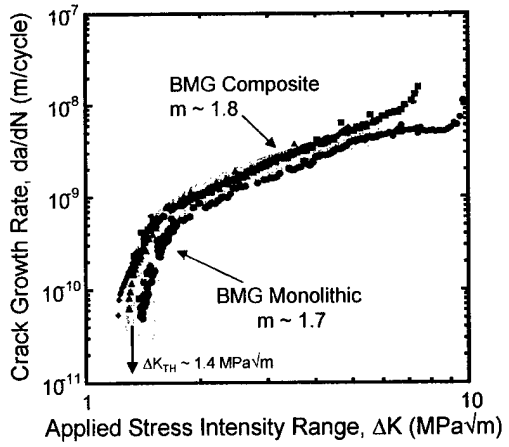

Figure 12: Fatigue crack-growth behavior of monolithic BMG (shown hatched) compared to a BMG composite with 25 vol.% Ti-Zr-Nb ductile β-phase.

any fatigue resistance compared to the matrix. As a result, none of the crack shielding mechanisms that typically increase fatigue crack-growth thresholds operate. Future studies will concentrate on mechanisms that may be employed to improve fatigue resistance. In the case of composites, the intent will be will be to study the volume fraction and morphology of the second phase in order to determine optimum distributions for improved fatigue resistance.

Environmental and Hydrogen Effects

The structural reliability of engineering materials may be significantly degraded by interactions with the surrounding environment. Environmentally-enhanced failures are insidious and depend sensitively on the synergistic interaction of material composition, mechanical loading conditions and the chemistry of the environmental species. Hydrogen in many environments represents an effective embrittling species and its effect on reducing ductility and fracture toughness has been extensively studied. However, the fundamental mechanisms of embrittlement remain largely unresolved in structural metallics.

In our previous program, characterization and modeling efforts were aimed at studying the effects of a number of environments on deformation, fracture resistance and subcritical-crack growth behavior in BMG's and their composites. These are essential elements for life prediction and fracture control schemes for structural materials as well as to provide guidelines for the development of new materials with improved reliability. To date, we have investigated the effects of hydrogen on the atomic relaxation processes that determine the glass transition temperature and crystallization kinetics, together with a variety of mechanical properties (indentation resistance, fracture toughness and fatigue crack-growth behavior) as described below [6,10,11,12,15,18]:

Relaxation Time and Viscosity

Dynamic mechanical analysis (DMA) was carried with frequency scans in the glass transition region. Representative DMA results of the as-received specimen are shown in Figure 13 where loss (E") modulus is plotted as a function of frequency. At each temperature, the loss modulus, which is related to the energy dissipation taking place in the atomic rearrangement process towards equilibrium configuration, shows a peak. The peak occurs when the laboratory time scale (inversely proportional to the applied frequency) becomes comparable to the relaxation time during frequency scan. Therefore, the average relaxation time (τ) can be obtained approximately from the frequency (ω_p) at which the loss factor exhibits a peak by:

$$\tau = \frac{1}{\omega_p}$$

At low temperatures, the peak of loss factor spectrum is not clearly discernible. With increasing temperature, however, dispersion behavior became more pronounced and the peak frequency was progressively shifted to higher frequencies indicating progressively shorter relaxation times with increasing temperature. For small departures from equilibrium and over limited temperatures, the temperature dependence of the relaxation time can be approximated by an Arrhenius expression with an apparent activation energy of Q:

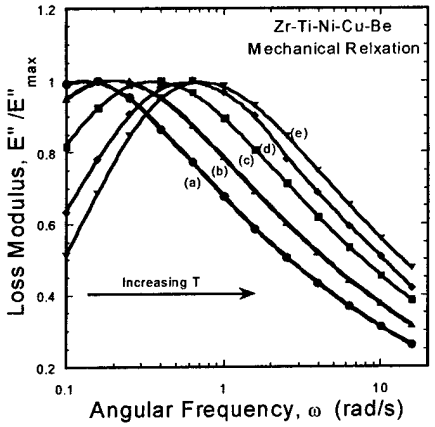

Figure 13: Normalized Loss (E''/E''_{max}) modulus as a function of angular frequency at various temperatures around the glass transition region: (a) 350, (b) 355, (c) 360, (d) 365, (d) 370°C.

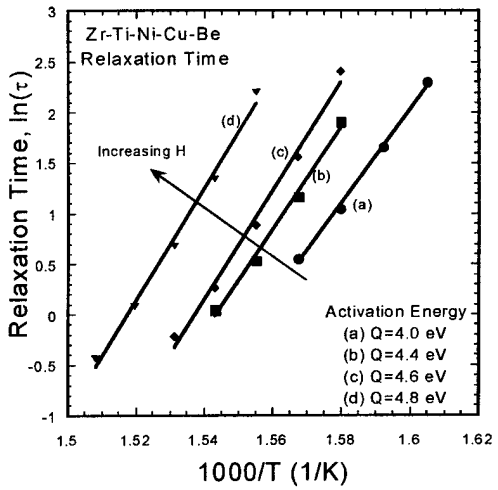

Figure 14: Relaxation time as a function of temperature for as-received (a) and hydrogen-charged specimens (b-d): (a) as-received (H_V=5.2 GPa), (b) H_V=5.41 GPa, (c) H_V=5.84 GPa, (d) H_V=6.63 GPa. Note that the degree of hydrogen charging is presented as Vickers hardness measured after charging.

$$\tau = \tau_o \exp\left(\frac{Q}{RT}\right)$$

The relaxation times obtained from the loss factor spectra are presented as a function of temperature for both as-received and hydrogen-charged specimens in Figure 14. An apparent activation energy of relaxation was obtained by measuring the slope. As shown in Figure 14, hydrogen charging progressively increases the magnitude and activation energy of the relaxation time. Since the measurements were made around the glass transition region, this relaxation time scale corresponds to that of viscous flow or structural relaxation responsible for the glass transition [16,17]. Therefore, hydrogen charging retards the atomic rearrangement process for viscous flow resulting in longer relaxation times and higher viscosity. These results are consistent with the progressively increasing glass transition temperatures with hydrogen charging in calorimetry measurements [15,18]

Crystallization Kinetics

In order to examine the effects of hydrogen on crystallization kinetics in detail, isothermal annealing was performed between the glass transition and onset of crystallization temperature by heating the sample in the DSC to a desired temperature with a fast heating rate (80 K/min) and letting the system crystallize isothermally. By integrating an exothermic peak corresponding to a crystallization event, the time required for a fixed amount of crystallization was obtained at each annealing

temperature. At a given annealing temperature, the charged specimen needed longer time ($t_{0.5}$) for 50 % crystallization compared to the as-received specimen. The temperature dependence of the rate of crystallization (~1/ $t_{0.5}$) can be approximated by an Arrhenius expression:

$$\frac{1}{t_{0.5}} \propto \exp\left(-\frac{Q}{RT}\right)$$

where Q is an apparent activation energy of crystallization. Although the overall rate of crystallization is retarded over the entire annealing temperature range, the activation energy was similar. Similar trends were observed for the secondary crystallization event.

Although direct correlation of viscosity to crystallization kinetics is not clear since the temperature range employed in this study (674 ~ 719 K) falls into the regime where the decoupling of diffusion of mid-sized and small atoms occurs from the viscosity, increased viscosity is likely to have retarding effects on crystallization through possibly retarded mobility of large atoms (Zr and Ti) whose time scale of diffusion still scales with that of viscous flow [19].

Effects of Hydrogen on Fracture and Fatigue Properties

As noted above, hydrogen charging significantly increased the glass transition and crystallization temperatures indicating significant effects on atomic relaxation and diffusion processes. Fracture toughness was also significantly degraded [12,15]. However, fatigue crack-growth rates were significantly retarded with hydrogen charging and fatigue threshold values were increased markedly (Fig. 15). The effect is associated with increases in fatigue crack closure in hydrogen charged samples.

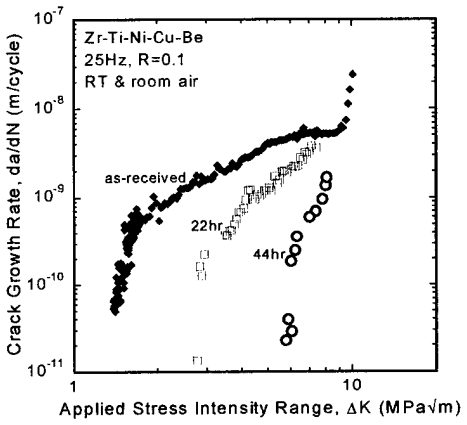

Figure 15: Fatigue crack-growth rates are retarded after hydrogen charging, however, fracture toughness values decrease. Decreased fatigue crack-growth rates are associated with increasing levels of crack closure.

The intent of our continuing research will therefore be to identify microstructural changes associated with hydrogen and other deleterious environmental species and to explain their effect on deformation, fracture resistance and subcritical crack-growth behavior.

Acknowledgement/Disclaimer

This work was supported (in part) by the Air Force Office of Scientific Research, USAF, under grant/contract number AF-F49620-98-1-0260-P00003. The views and conclusions contained herein are those of the authors and should not be interpreted as necessarily representing official policies or endorsements, either expressed or implied, of the Air Force Office of scientific Research or the U.S. Government.

PERSONNEL SUPPORTED ON PREVIOUS AFOSR PROGRAM

Katharine Flores	(Ph.D.)	Fellowship student – partial support
Daewoong Suh	(Ph.D.)	Fellowship student – partial support
Wendy Wright	(Ph.D.)	Fellowship student – partial support
Reinhold H. Dauskardt		Associate Professor (PI)
William D. Nix		Professor (Co-PI)

PUBLICATIONS

Publications resulting from our AFOSR program are listed below as references: 3 – 13, 15, 18.

REFERENCES

1. F. Spaepen, D. Turnbull, *Scripta Metallurgica*. 8 (1974) 563.
2. H. J. Leamy, H. S. Chen, T. T. Wang, *Metallurgical Transactions*. 3 (1972) 699.
3. W. J. Wright, R. Saha, and W. D. Nix, "Deformation Mechanisms of the ZrTiNiCuBe Bulk Metallic Glass," Materials Transactions, JIM, 2001. In press.
4. W.J. Wright, W.D. Nix and R.B. Schwarz, "Serrated Plastic Flow in Bulk Metallic Glasses," Materials Science and Engineering A, 2001. In press.
5. R. Huang, Z. Suo, J.H. Prevost and W.D. Nix, "Inhomogeneous Deformation in Metallic Glasses," Journal of Mechanics and Physics of Solids, 2001. In review.
6. K. M. Flores, D. Suh, and R. H. Dauskardt, in Bulk Metallic Glasses, edited by A. Inoue, W. Johnson, and C. T. Liu, Proc. MRS Annual Meeting, 554, Boston, MA, 1999. 355 – 360.
7. K. M. Flores and R. H. Dauskardt, "Mean stress Effects on Flow Localization and Failure in a Bulk Metallic Glass," Acta Metallurgica et Materialia, 49, 2001. In press.
8. K. M. Flores and R. H. Dauskardt, Journal of Materials Research, 14 [3] 638-643, 1999.
9. K. M. Flores and R. H. Dauskardt, "Mode II Fracture of a Zr-Based Bulk Metallic Glass," Scripta Materialia, 2001. In review.
10. K. M. Flores, D. Suh, R. Howell, P. Asoka-Kumar, P.A. Sterne, and R. H. Dauskardt, "Flow and Fracture of Bulk Metallic Glass Alloys and Their Composites," Materials Transactions, JIM, 2001. In press.
11. K. M. Flores, D. Suh, P. Asoka-Kumar, P.A. Sterne, R. Howell, and R. H. Dauskardt, "Characterization of Free Volume in Bulk Metallic Glass Using Positron annihilation Spectroscopy," Journal of Materials Research, 2001. In review.
12. D. Suh and R. H. Dauskardt, "The Effects of Pre-Charged Hydrogen on the Mechanical and Thermal Behavior of Zr-Ti-Cu-Ni-Be Bulk Metallic Glass Alloys," Materials Transactions, JIM, 42 [4], 2001. In press.
13. K. M. Flores and R. H. Dauskardt, Scripta Materialia, 41 [9] 937-943, 1999.
14. C. J. Gilbert, V. Schroeder, and R. O. Ritchie, Met. Trans. A, v. 30, 1739 (1999).
15. D. Suh and R. H. Dauskardt, Scripta Materialia, 42 [3] 233-240, 2000.
16. C.T. Moynihan, in *Assignment of the Glass Transition*, edited by R.J. Seyler (ASTM STP 1249), American Society for Testing and Materials, Philadelphia, p.32 (1994).
17. C.A. Angell, *Chem. Rev.* 90 (1990) 523.
18. D. Suh and R.H. Dauskardt, *Mat. Sci Eng.* (2001). In press.

19. A. Masuhr, T.A. Waniuk, R. Busch and W.L. Johnson, *Phys. Rev. Lett.* 82, 2290 (1999).

INTERACTIONS

Research was undertaken in collaboration with Prof. W. Johnson at CALTECH. Material for this work was provided by Amorphous Technologies International, Laguna Niguel, California, and by Howmet Research Corporation, Whitehall, Michigan.

CONSULTATIVE FUNCTIONS
None

TRANSITIONS
None

NEW DISCOVERIES

Adiabatic heating directly imaged during plastic deformation in bulk metallic glasses.

Awards Received

W. D. Nix, Alpha Sigma Mu Lecturer and Distinguished Life Membership, ASM International, 2000.
W.D. Nix, Honorary Doctor of Engineering Degree, Colorado School of Mines, (2001).

Transitions

None.